A Key Leakage Preventive White-box Cryptographic Implementation

Seungkwang Lee, Nam-su Jho, Myungchul Kim

Information Security Research Division, ETRI
skwang@etri.re.kr

Abstract. A white-box cryptographic implementation is to defend against white-box attacks that allow access and modification of memory or internal resources in the computing device. In particular, linear and non-linear transformations applied to this table-based cryptographic implementation are used to prevent key-dependent intermediate values from being seen by white-box attackers. However, it has been shown that there is a correlation before and after the linear and non-linear transformations so that even a gray-box attacker can reveal secret keys hidden in a white-box cryptographic implementation. In this paper, we focus on the problem of linear transformations including the characteristics of block invertible binary matrices and the distribution of intermediate values. Based on our observation, we find out that a random byte insertion in the intermediate values before linear transformations can eliminate a problematic correlation to the key, and propose our white-box AES implementation using this principle. Our proposed implementations reduce the memory requirement by at most 33 percent compared to the masked implementations and also slightly reduce the number of table lookups. In addition, our method is a non-masking technique and does not require a static or dynamic random source, unlike the existing gray-box (power analysis) countermeasures.

Keywords: White-box cryptography, power analysis, differential computation analysis, linear transformations, countermeasure.

1 Introduction

From a secret key point of view, a block cipher can be seen as a secret bijective function between a plaintext set and a ciphertext set. One possible implementation of this function is a lookup table of the ciphertext for each of its corresponding plaintext. Since implementing a cipher as one lookup table is impractical because of its huge size, it is usually implemented as a series of lookup tables. This table-based implementation is also used in the white-box cryptographic implementation so that a secret key is not revealed by a white-box attacker observing internal memory and computing resources. The important thing to remember over here is that the white-box cryptography generates key-instantiated lookup tables and protects each table with linear and non-linear transformations in order to prevent a key leakage from lookup values. Due to these transformations, a white-box attacker has been supposed to be unable to recognize a secret key via static or dynamic analysis.

So far, this white-box cryptography has been exploited by highly skilled attacks except for code lifting attacks [20] that steal the entire lookup table. For example, after the first two white-box DES (WB-DES) [6] and AES (WB-AES) [5] implementations were published, a number of practical cryptanalysis techniques [7][21] [1][12][15] have been introduced to extract the secret key from the white-box lookup tables. Many variants of WB-DES and WB-AES implementations [4][23] [8][11][13] were proposed and many were known to be practically broken [16][17]. Recently, Differential Fault Analysis (DFA) [18] was introduced, where an attacker is able to inject a fault at a desired location in memory. What they have in common is that those white-box attacks rely on an in-depth understanding of a target implementation so that an attacker is able to gain read/write access to precise internal states during the execution. Thus commercial white-box cryptography focuses on making a barrier to the full control of an attacker and is often combined with additional software-based protection methods including control flow obfuscation, tamper resistance, device binding and anti-debug protections. An explanation of these protections, primarily taking into account an untrusted environment, could be that the white-box implementation was considered to be able to defend against gray-box attacks, also known as side-channel attacks.

In contrast to white-box attacks, gray-box attacks are dependent on non-invasive information such as timing and power consumption obtained while a target device performs cryptographic operations. Simple Power Analysis (SPA) is a timing-based attack that visually interprets power traces over time. For example, SPA can analyze exponentiation algorithms by distinguishing the square and multiply operations. On the other hand, Differential Power Analysis (DPA) [9] is based on power consumption and this is one of the most well-known techniques to reveal the secret key imbedded in IC cards. Specifically, DPA is generally based on the fact that power consumption of a device is proportional or inversely proportional to the Hamming weight (HW) of data it processes. Thus a power analysis attacker collects a number of power traces with random plaintexts and finds a correct key that computes hypothetical values most highly correlated to the collected traces at a particular point. Currently, one critical issue for the white-box implementation is that it is successfully attacked by power analysis. This means linear and non-linear transformations applied to lookup tables have no effect on hiding key-sensitive intermediate values. This fact violates the reason for the white-box cryptography which is initially said to be secure even in the white-box attack model, where an attacker has full control over everything.

In light of this vulnerability, finding software countermeasures to counteract power analysis has become essential for the further growth of white-box cryptography. Here are some examples. First, control flow obfuscation shuffles the order of table lookup only if it does not make any difference in the final result. The use of run-time random source for the large enough disarrangement and the re-ordering overhead are costly. Second, table location randomization is used to counteract address-based DPA, named Differential Computation Analysis (DCA) [2]. Among many variants of DPA including Correlation Power Analysis (CPA) [3], DCA is a more skilled attack that uses software execution traces containing both sensitive data and memory address accesses; for this reason, DCA shows better analysis performance, but is often considered a white-box attack. In this sense, one may try to disperse the tables at random locations. Of course, it is useless if value-based DCA is mounted. Third, adding an arbitrary number of dummy lookups can be one of the disarrangement methods to randomize the time instance at which the target intermediate value is computed for each execution. However, all these run-time randomization methods are expensive and can always be compromised by a white-box attacker. Last but not least, there is a masked white-box implementation [10] for protecting against DCA and other DPA-like attacks. The key idea behind is to apply masking to sensitive intermediate values before encoding them during the table generation. However, this method did not address the fundamental reason for the imbalance pertaining to the encoding but applied the existing masking to eliminate the vulnerability at a high cost.

1.1 Our contribution

- We find out that the key leakage after linear transformations is largely due to the balanced distribution of intermediate values.
- We also find out that a random byte insertion in the intermediate value before linear transformations prevents the key leakage. Furthermore, our experimental results show that inserting position does not make difference and inserting more than one byte provides no additional effect.
- We provide a non-masking design of WB-AES based the above principle without the need for static or dynamic random sources. The memory requirement and the number of lookups are decreased compared to masked WB-AES implementations.

1.2 Organization of the Paper

The rest of this paper is organized as follows. Section 2 reviews some basic concepts including power analysis, the principle of a white-box cryptographic implementation, and the key leakage issue. In Section 3, we analyze the invertible linear transforms used in the white-box cryptography to see why the key-dependent intermediate values are still correlated to the key even after linear transformations. Based on this analysis, we propose our solution resistant to DCA and DPA-like attacks in Section 4. Specifically, a WB-AES implementation is newly implemented for concrete demonstration. We then evaluate its security and performance in Section 5. Finally, Section 6 concludes this paper.

2 Background

In this section, we introduce the basic concept of power analysis and a WB-AES implementation first appeared in [5], and then investigate key leakage points with the Walsh transforms.

2.1 Power Analysis

Gray-box attacks, which recently attacked white-box cryptography, are precisely power analysis such as DPA and CPA. DCA attacks can not be classified into gray-box attacks in the correct sense because of the direct access to memory in the process of collecting software execution traces. Of course, DPA and CPA attack efficiency is greatly increased when combined with DCA since there is no measurement noise in the software execution traces, unlike the power consumption traces.

After collecting the traces with random plaintexts, DPA and CPA perform statistical analysis in different ways. DPA uses the selection function D to split the collected traces into two sets based on the attacker's hypothetical values. If the attacker's hypothetical key is correct (the hypothetical value is correct), then the separation of the traces by D is also accurate and there will be a peak in the differential trace.

In contrast, CPA uses a leakage model including the Hamming weight (HW) and the Hamming distance instead of the selection function D. When attacking a white-box implementation, the bit (mono-bit) model is appropriate because HW-based CPA attacks are unlikely to be successful due to the disturbed HW by linear and non-linear transformations. Given N power traces $V_{1..N}[1..\kappa]$ containing κ samples each, CPA will estimate the power consumption at each point of each trace using attacker's hypothetical intermediate value. For K different key candidates, let $\mathcal{E}_{n,k^*}$ ($1 \le n \le N$, $0 \le k^* < K$) denote the power estimate in the n^{th} trace with the hypothetical key k^*. To measure a correlation between hypothetical power consumption and measured power traces, the estimator r is defined as follows [14]:

$$r_{k^*,j} = \frac{\sum_{n=1}^{N}(\mathcal{E}_{n,k^*} - \overline{\mathcal{E}_k^*}) \cdot (V_n[j] - \overline{V[j]})}{\sqrt{\sum_{n=1}^{N}(\mathcal{E}_{n,k^*} - \overline{\mathcal{E}_k^*})^2 \cdot \sum_{n=1}^{N}(V_n[j] - \overline{V[j]})^2}},$$

where $\overline{\mathcal{E}_k^*}$ and $\overline{V[j]}$ are sample means of $\mathcal{E}_k^*$ and $V[j]$, respectively. If there exists a correlation, a noticeable peak will be found in the correlation plot for the correct key. An explanation of successful CPA on the white-box cryptographic implementation could be that attacker's correct hypothetical value will correlate to the target table lookup value.

2.2 WB-AES Implementation

In this section, we briefly explain the initial WB-AES implementation [5]. For the WB-AES implementation with a 128-bit key, the AES algorithm is re-written as follows:

```
state ← $plaintext$
for $r = 1$ to 9 do
    ShiftRows(state)
    AddRoundKey(state, $\boldsymbol{k}^{r-1}$)
    SubBytes(state)
    MixColumns(state)
ShiftRows(state)
AddRoundKey (state, $\boldsymbol{k}^{9}$)
SubBytes(state)
AddRoundKey(state, $k^{10}$)
$ciphertext$ ← state,
```

where k^r means the 4×4 round key matrix for round r, and $\boldsymbol{k}^r_{i,j}$ indicates that the ShiftRows is applied to $k^r_{i,j}$. A WB-AES implementation is currently based on the table-based implementation which combines the above operations except for ShiftRows into a set of lookup tables and applies linear and non-linear transformations. Linear transformations use two types of invertible matrices. One is multiplied to partial MixColumns outputs and the other is multiplied to each round input byte. Non-linear transformations consist of two 4-bit concatenated random bijections to reduce the total table size. More specifically, if 8-bit random bijections are used in non-linear transformations, the XOR lookup table size will increase significantly because an XOR table has to take two 8-bit inputs instead of two 4-bit ones. An encoding throughout the paper means the linear and non-linear transformations. On the condition that there is no external encoding (done by *TypeI*) for better comparability with non-WB-AES implementations, we need four types of the lookup tables: *TypeII*, *TypeIII*, *TypeIV* and *TypeV*. From now on, we explain how to generate them.

TypeII. The lookup values of *Type* $II^r_{i,j}$ provide the encoded result of AddRoundKey, SubBytes and decomposed multiplications of MixColumns, where $0 \leq r \leq 9$, and $0 \leq i, j \leq 3$. The first step of generating *TypeII* is to combine AddRoundKey and SubBytes into *T-boxes*, 160 8×8 lookup tables, as follows:

$$\begin{aligned}&T^r_{i,j}(p) = S(p \oplus \boldsymbol{k}^{r-1}_{i,j}), \qquad 0 \leq i,j \leq 3, 1 \leq r \leq 9,\\ &T^{10}_{i,j}(p) = S(p \oplus \boldsymbol{k}^{9}_{i,j}) \oplus k^{10}_{i,j}, 0 \leq i,j \leq 3.\end{aligned}$$

Note that *TypeII* uses T^1 - T^9 and *TypeV* uses T^{10} later. What is important over here is that we must decode the input of *TypeII* from round 2 based on the index change due to ShiftRows since it is encoded output of the previous round. On the other hand, the input to *TypeII* in the first round is not required to be decoded because we do not use the external encoding. Let $L^r_{i,j}$ denote 144 (=9×4×4) 8×8 binary invertible matrices used to linearly transform each byte of the round out, where $r \in$ [1, 9], $0 \leq i,\ j \leq 3$. In round $r \geq 2$, the inverse linear transformation (after inverse non-linear transformation) on the encoded *TypeII* input p' at the index $\{i,\ j\}$ is performed as follows:

1. Adjust the proper index after ShiftRows to find the corresponding inverse matrix of the linear transformation; $\{i,\, j'\} \leftarrow \{i,\, (j+i) \bmod 4\ \}$
2. $p \leftarrow (L^{r-1}_{i,j'})^{-1} \cdot p'$.

Then we know that $T^r_{i,j}(p)$ gives us an input x to the MixColumns step except for $T^{10}_{i,j}(p)$ because there is no MixColumns in the final round. Let's decompose the matrix multiplication with a column vector in MixColumns as follows:

$$\begin{pmatrix} 02\ 03\ 01\ 01 \\ 01\ 02\ 03\ 01 \\ 01\ 01\ 02\ 03 \\ 03\ 01\ 01\ 02 \end{pmatrix} \begin{pmatrix} x_0 \\ x_1 \\ x_2 \\ x_3 \end{pmatrix} = \\ x_0 \begin{pmatrix} 02 \\ 01 \\ 01 \\ 03 \end{pmatrix} \oplus x_1 \begin{pmatrix} 03 \\ 02 \\ 01 \\ 01 \end{pmatrix} \oplus x_2 \begin{pmatrix} 01 \\ 03 \\ 02 \\ 01 \end{pmatrix} \oplus x_3 \begin{pmatrix} 01 \\ 01 \\ 03 \\ 02 \end{pmatrix} .$$

For four terms y_0, y_1, y_2, y_3 at the right-hand side, we define Ty_i tables:

$$\begin{aligned} Ty_0(x) &= x \cdot [02\ 01\ 01\ 03]^T \\ Ty_1(x) &= x \cdot [03\ 02\ 01\ 01]^T \\ Ty_2(x) &= x \cdot [01\ 03\ 02\ 01]^T \\ Ty_3(x) &= x \cdot [01\ 01\ 03\ 02]^T. \end{aligned}$$

The next step is to perform linear transformations on $Ty_{i\in\{0,1,2,3\}}(x)$ with a given invertible 32×32 matrix M, conduct non-linear transformations and store them in *TypeII* as illustrated in Fig 1. During the execution of WB-AES, its lookup values will contain 4-byte outputs and thus the intermediate values after visiting *TypeII* will be store in a 4×4×4 matrix. Of course, this dimensional structure can be different depending on the programmer's choice.

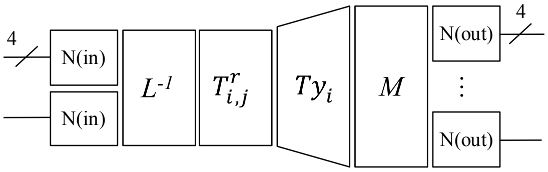

Fig. 1: A schematic diagram of *TypeII* generation. N: non-linear transformations.

TypeIII. During the *TypeIII* generation (Fig. 2), we perform the inverse linear transformation with M^{-1} and apply the linear transformation with L. These two linear transformations result in one byte size of the *Type II* input in the next round. After combining intermediate values by looking up *TypeIV_III*, the linear transformation by M is canceled out and the linear transformation by L protects the round output in the state matrix. In turn, this will be canceled out in *TypeII* input decoding. After visiting *TypeIII*, we have the intermediate values in a 4×4×4 matrix.

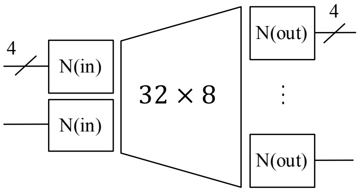

Fig. 2: A schematic diagram of *TypeIII* generation.

TypeIV. This performs XOR operations in order to combine intermediate values. Thus *TypeIV* depicted in Fig. 3 is visited after *TypeII* or *TypeIII* lookups; we call them *TypeIV_II* and *TypeIV_III* which are used to XOR the lookup values of *TypeII* and *TypeIII*, respectively. *TypeIV_II* and *TypeIV_III* combine 4×4×4 intermediate values into a 4×4 state matrix.
All two 4-bit inputs to be XORed must be linearly transformed at the same offset of the same invertible matrix so that we do not need to linearly transform the input when generating *TypeIV* because it satisfies the distributive property of multiplication over addition. Fig. 4 and Fig. 5 simplify the lookup flows of *TypeIV* following *TypeII* and *TypeIII*.

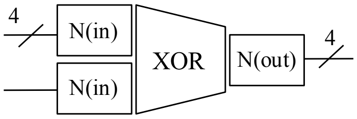

Fig. 3: A schematic diagram of *TypeIV* generation.

TypeV. This includes T^{10} and is looked up in the final round. Because there is no MixColumns *TypeIV* is not followed. Also, the lookup values of *TypeV* depicted in Fig. 6 are not encoded because they are the ciphertext, and as stated previously we assume that there is no external encoding. Then, an AES encryption can be performed by only ShiftRows and table lookups of these four types of lookup tables.
This WB-AES implementation has three key leakage points that could be successfully analyzed by gray-box attacks. First, an attacker can perform a DPA

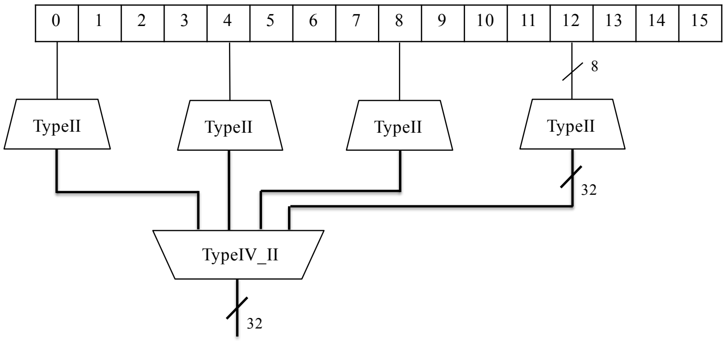

Fig. 4: *TypeII* and *TypeIV_II* lookups.

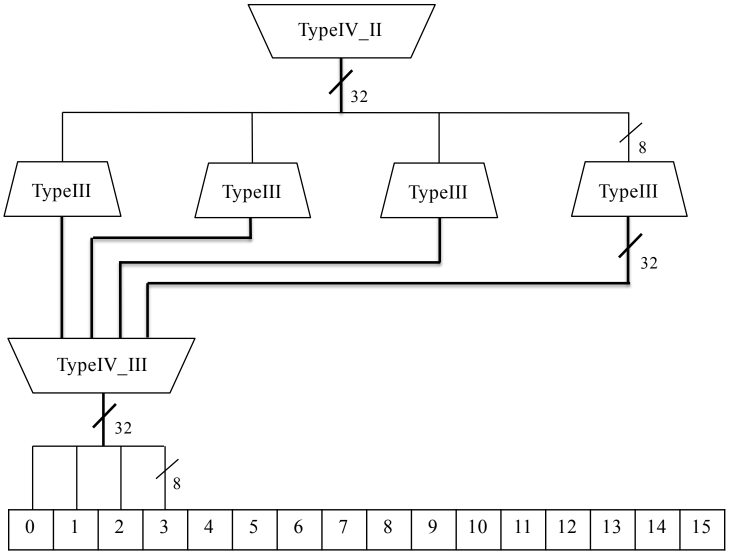

Fig. 5: *TypeIII* and *TypeIV_III* lookups.

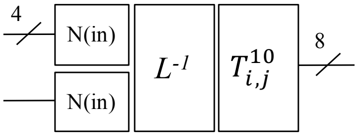

Fig. 6: A schematic diagram of *TypeV* generation.

or CPA attack on the SubBytes output, that is the *TypeII* output, in the first round. Then it requires to test 2^8 candidates for each subkey of the first round key provided that there is no protection for key leakage. Second, as explained in [10], the final round input (or the ninth round output) can be attacked with 2^{16} candidates for each subkey of the final round key due to the absence of MixColumns. Lastly, it is not impossible to attack the first round output by searching 2^{32} candidates for each 4-byte column vector of the first round key matrix. Then attacker's target values will be *TypeIV_II* or *TypeIV_III* outputs in the first round. In the next section, we explain the use of the Walsh transforms to detect key leakages and demonstrate the key leakages in this WB-AES implementation.

2.3 Detecting Key Leakage by the Walsh Transforms

In addition to common power analysis techniques such as DPA and CPA (or DCA) we can quantify or visualize a correlation using the Walsh transforms if a target lookup table is given. To understand how the Walsh transform can be used to quantify a correlation between the input and output of a target lookup table, we use the following definitions from [19].

Definition 1. *Let $x = \langle x_1, \ldots, x_n \rangle$, $\omega = \langle \omega_1, \ldots, \omega_n \rangle$ be elements of $\{0,1\}^n$ and $x \cdot \omega = x_1\omega_1 \oplus \ldots \oplus x_n\omega_n$. Let $f(x)$ be a Boolean function of n variables. Then the Walsh transform of the function $f(x)$ is a real valued function over $\{0,1\}^n$ that can be defined as $W_f(\omega) = \Sigma_{x \in \{0,1\}^n} (-1)^{f(x) \oplus x \cdot \omega}$.*

Definition 2. *Iff the Walsh transform W_f of a Boolean function $f(x_1, \ldots, x_n)$ satisfies $W_f(\omega) = 0$, for $0 \leq HW(\omega) \leq m$, it is called a balanced m^{th} order correlation immune function or an m-resilient function.*

Then we know that $W_f(\omega)$ quantifies the imbalances in the encoding, and the large absolute value of $W_f(\omega)$ means the strong correlation between $f(x)$ and $x \cdot \omega$. Using this property of the Walsh transforms, we calculate the correlation between the table lookup values and hypothetical values.

Let's demonstrate the key leakage from the *TypeII* lookup value in the first round. Given a subkey $k^0_{0,2} = \mathit{0x}88$, and for every input value $p \in \mathrm{GF}(2^8)$, we know that

$$\begin{aligned} x &= S(p \oplus k^0_{0,j}) \\ y_0(x) &= \begin{bmatrix} 2 \cdot x \; x \; x \; 3 \cdot x \end{bmatrix}^T \end{aligned}$$

where S represents the AES SubBytes and the multiplication by 2 is implemented as a 1-bit left shift followed by a conditional ($\oplus$ 0x1B) if the MSB of the operand was 1. Then $f(x)$ here denotes *TypeII* lookup values which are computed by linear and non-linear transformations on $y(x)$, and we have 32 Boolean functions $f_{i \in \{1,\ldots,32\}}(x)$: $\{0,1\}^8 \rightarrow \{0,1\}$. To find a correct key, we calculate the Walsh transforms W_{f_i} and sum all the imbalances for each key candidate and ω such that HW(ω) = 1 as follows:

$$\Delta^f_{k\in\{0,1\}^8} = \sum_{\omega=1,2,4,\ldots,128}\ \sum_{i=1,\ldots,32} |W_{f_i}(\omega)|.$$

The reason why we only select ω of HW(ω) = 1 is that the HW-based key leakage model is not effective to detect the correlation between the in/output of the encoding.

The Walsh transforms and their sum of all imbalances are given in Fig. 7. As we can see in Fig. 7a, the Walsh transforms with $\omega = 4$ of the correct key ($\mathit{0x}88$) produce 0 except two points; the W_{f14} and W_{f16} of the correct key are -128, and their absolute value (128) is the most highest value. In contrast the maximum and the average values of $|W_{f_i}(\omega)|$ of wrong key candidates are 56 and about 13.13 (the standard deviation is about 9.35), respectively. This gives us that $f_{14}(\cdot)$ and $f_{16}(\cdot)$ cause key leakages and thus power analysis using the 3^{rd} bit (when the LSB is the 1^{st} bit) of attacker's hypothetical SubBytes outputs is able to recover this subkey. $\Delta^f_{k=\mathit{0x}88}$ is 256 (= $|-128|$ + $|-128|$) which is obviously distinguishable from that of other key candidates as shown in Fig. 7b while $\Delta^f_{k\neq \mathit{0x}88}$ are about 2900-3700. This simply shows us how to use the sum of all imbalances for recovering the correct key.

In the similar way, we can detect a key leakage at the final round input. In this scenario, we give the first subkey of the ninth round key ($\mathit{0x}54$) and let the attacker guess the first subkey ($\mathit{0x}13$) of the final round. Given a subbyte of the ciphertext, x becomes the attacker's hypothetical input value and 8 Boolean functions $f_{i\in\{1,\ldots,8\}}(x)$: $\{0,1\}^8 \rightarrow \{0,1\}$ indicate the encoded input to *TypeV*. On the condition that there is no external encoding on the ciphertext and the attacker knows the first subkey of the ninth and final round keys, $\Delta^f_{k=\mathit{0x}13}$ in the final round is 4096; this is much smaller than $\Delta^f_{k\neq \mathit{0x}13}$ in the range 25900 - 26500 as shown in Fig. 8. In the following section, we analyze the linear transformations used in the white-box lookup table generation, and provide a clue for a secure implementation.

3 Analysis of Linear Transformations

3.1 Key Leakage Statistics after Linear Transformations

In this section, we begin with an experimental result of a key leakage at the linear transformation demonstrated by the sum of imbalance depicted in Fig. 9, where the Walsh transforms use

$$f(x) = M \cdot y_{i\in\{0,1,2,3\}}(x),$$

for x of each y_i computed from four subkeys, the 9^{th} to 12^{th} subkeys ($\mathit{0x}88$, $\mathit{0x}99$, $\mathit{0x}$AA, $\mathit{0x}$BB) of the first round in this experiment, and a 32×32 binary invertible matrix M. Unlike in the case of Fig. 7b of a key leakage from the linear

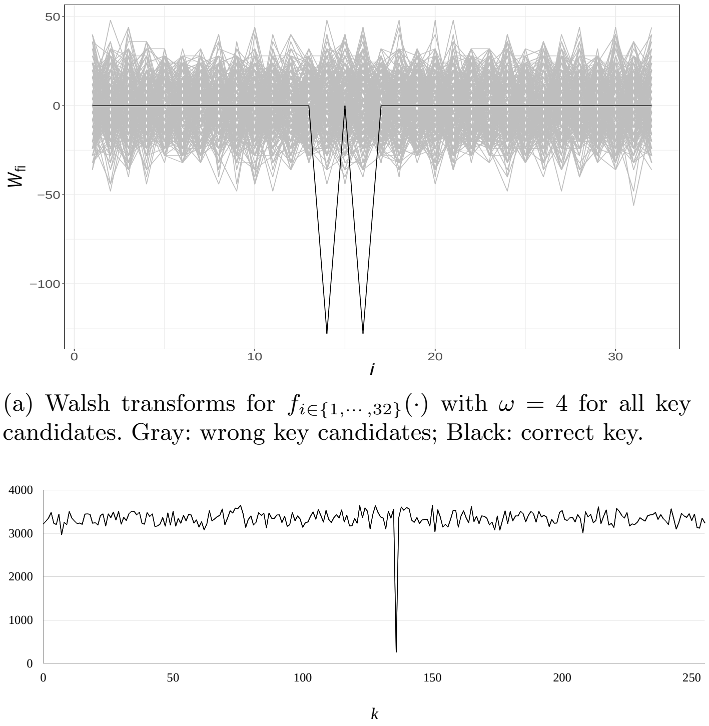

(a) Walsh transforms for $f_{i\in\{1,\cdots,32\}}(\cdot)$ with $\omega = 4$ for all key candidates. Gray: wrong key candidates; Black: correct key.

(b) Sum of all imbalances for all key candidates.

Fig. 7: Key leakage detection using the Walsh transforms.

and non-linear transformations, this shows a key leakage from linear transformations without non-linear transformations. We can see that linear transformations with M can hide three subkeys $0x$88, $0x$AA, and $0x$BB, but expose one subkey $0x$99 from $y_1(x)$. This gives us two facts. First, as we will show later in this section, linear transformations produce well-balanced output with an overwhelming probability, but this is not always guarantee a reliable protection on secret keys. Second, the correct key can be recovered by the Walsh transforms even if its sum of imbalances is 0 indicating no correlation when it is distinguishable.

TABLE 1 and Fig. 10 show our experimental results of linear transformations on $y_{i\in\{0,1,2,3\}}(x)$ using 1000 randomly generated invertible matrices. For HW(ω) = 1, $Wf_i(\omega)$ = 0 with approximately 99.7% and 0.3 % of $Wf_i(\omega)$ = 256; the average of $|W_{f_i}(\omega)|$ is approximately 0.7. We will show later there is no other $Wf_i(\omega)$ values. Here, both cases (0 and 256) will lead to two different types of key leakages due to the distinguishable Walsh transform value and the noticeably high correlation coefficient, as pointed out previously. Recall that there are 8 values of $\omega \in$ GF(2^8) such that HW(ω) = 1 and y_0 - y_3 output 32-bit values for x, and thus 1024 Wf_i will be tested to see if there exists a key leakage from the linear transformation using a matrix M. Consequently, there probably exist

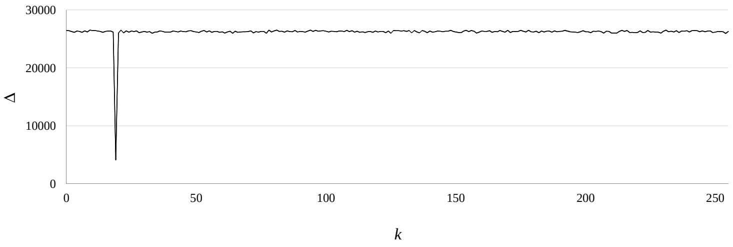

Fig. 8: Sum of the imbalance for all key candidates in the final round input.

Table 1: Experimental results of linear transformations with 1000 randomly generated block invertible matrices. k^c: correct key.

	Vectors to be transformed			
Number of	y_0	y_1	y_2	y_3
$Wf_i(\omega) = 0$	255,206	255,205	255,309	255,203
$Wf_i(\omega) = 256$	794	795	691	797
$\Delta^f_{k^c} = 0$	475	489	520	464
$\Delta^f_{k^c} = 256$	333	307	316	343
$\Delta^f_{k^c} = 512$	132	144	122	146
$\Delta^f_{k^c} > 512$	60	60	42	47

about 3 peaks of the correct key distinguishable from wrong key candidates. Each of y_0, y_1, y_2, and y_3 shows around 1/2 probability of $\Delta^f_{k^c} = 0$, and only about 5% of matrices do not leak any subkeys after linear transformations, where k^c means the correct key. In most cases, 1-to-3 out of four subkeys are shown to be exposed.

From now on, we are going to analyze this problematic characteristic of the linear transformations that produce extreme Wf_i values of 0 or 256. The first thing we want to investigate is whether the invertible matrix is responsible for this matter.

3.2 Analysis of Block Invertible Square Matrix

In [5], the authors choose M as a non-singular matrix with submatrices of full rank with a reference to [22] for maximizing information diffusion. To begin with, we briefly review the definition of a block invertible square matrix.

Definition 3. *If all the blocks $B_{i,j}$ in a block matrix ${}^{n}_{m}M[{}^{p}B]$ are invertible, matrix M is called an $(m,\ n,\ p)$ block invertible matrix. Furthermore, if $m = n$, and M is invertible then M is called an $(m,\ p)$ block invertible square matrix,*

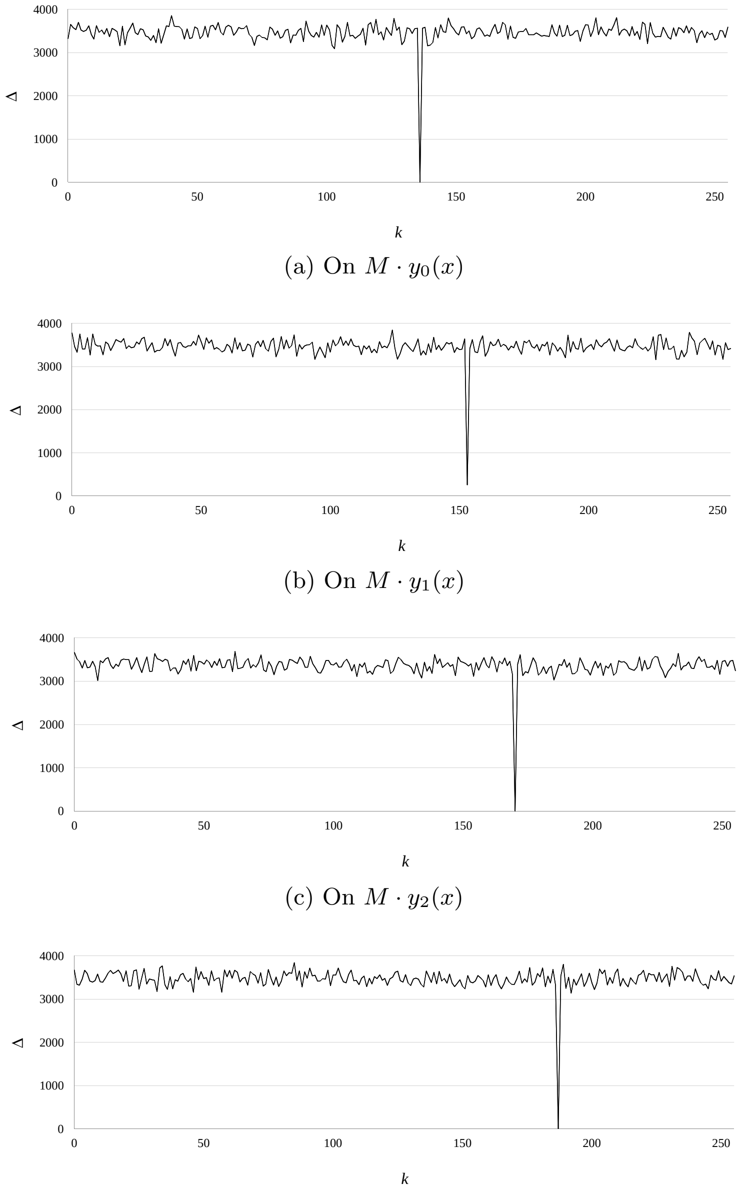

(a) On $M \cdot y_0(x)$

(b) On $M \cdot y_1(x)$

(c) On $M \cdot y_2(x)$

(d) On $M \cdot y_3(x)$

Fig. 9: Sum of the imbalance of $W_{f_i}(\omega)$ for all key candidates on each $y_{i\in\{0,1,2,3\}}(x)$ with only linear transformations.

where ${}^{n}_{m}M[{}^{p}B]$ *denotes an* $n \times m$ *matrix* M *with* nm/p^2 *blocks (submatrices),*

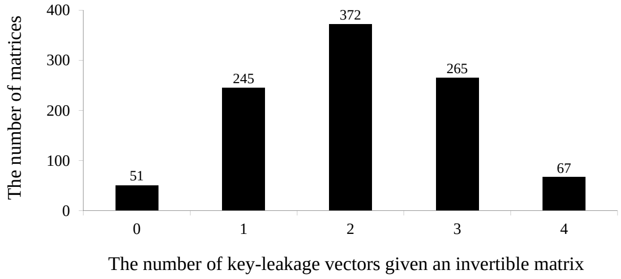

Fig. 10: The number of block invertible matrices (y-axis) vs. the number of key-leakage $y_{i\in\{0,1,2,3\}}$ given a block invertible matrix (x-axis).

and $B_{i,j}$ denotes the block in row i and column j of blocks [22].

Generating (n, 2) block invertible square matrices begins with a (2, 2) block invertible square matrix and extends by (4, 2), (6, 2), . . ., and repeats it $(n-2)/2$ times. The important point over here is that every 2×2 submatrix in a (n, 2) block invertible square matrix should be invertible by the definition and all 2×2 invertible matrices in GF(2) are as follows:

$$\begin{vmatrix}1&0\\0&1\end{vmatrix}\quad\begin{vmatrix}1&1\\1&0\end{vmatrix}\quad\begin{vmatrix}0&1\\1&1\end{vmatrix}\quad\begin{vmatrix}0&1\\1&0\end{vmatrix}\quad\begin{vmatrix}1&1\\0&1\end{vmatrix}\quad\begin{vmatrix}1&0\\1&1\end{vmatrix}$$

At a glance, the number of 1s in the 4 out of 6 matrices is greater than 0s. By the principle of constructing a block invertible square matrix, the HW of each row and column in an (n, 2) block invertible matrix will be greater than $n/2$. For example, let's assume that a (4, 2) matrix is initialized with

$$\begin{vmatrix}1&0\\0&1\end{vmatrix},$$

then its resulting matrix will be

$$\begin{vmatrix}1&0&1&0\\0&1&0&1\\1&0&1&1\\0&1&1&0\end{vmatrix}.$$

In the case of an initialization with

$$\begin{vmatrix}0&1\\1&0\end{vmatrix},$$

we will have

$$\begin{vmatrix}0&1&0&1\\1&0&1&0\\0&1&1&0\\1&0&1&1\end{vmatrix}.$$

During the generation of a (32, 2) matrix through this process, 1s appear more frequently. We have performed the following experiment to check if this over-weight HW of the invertible block square matrix is the main reason for key leakage. We randomly generated a balanced *non-invertible* 32×32 matrix M^b, such that $f(x) = M^b \cdot y_{i \in \{0,1,2,3\}}(x)$, where M^b has the HW of 16 for each row and column, and used it to compute the sum of imbalances. As shown in Fig. 11. there still exist key leakages from y_1 and y_2 with $\Delta^f_{k^c} = 256$. For this reason, we can conclude that the matrix HW itself is not the cause of key leakages from linear transformations.

3.3 Analysis of Key-dependent Intermediate Values

The next key-leakage point to be analyzed is y. From Definition 1 and 2, we know that a balanced correlation immune function is strongly dependent on the distribution of $f_i(x) \oplus x \cdot \omega$. Since a matrix characteristic is not responsible for the key leakage as we analyzed previously, the distribution of y is convinced to mainly decide the distribution of $f_i(x) \oplus x \cdot \omega$. Here recall that given a key-dependent value $x \in \mathrm{GF}(2^8)$ and 1000 randomly generated invertible matrices M, $W_{f_i}(\omega) = 0$ with approximately 99.7% while only 0.3% of $W_{f_i}(\omega) = 256$, where $\mathrm{HW}(\omega) = 1$. The following lemma explains the reason behind.

Lemma 1. *Assume that a 256×8 binary matrix* $\mathbf{H}$ *is defined as*

$$\mathbf{H} = \begin{bmatrix} h_{1,1} & h_{1,2} & \dots \\ \vdots & \ddots & \\ h_{256,1} & & h_{256,8} \end{bmatrix}$$

where i-th row vector $\mathbf{h}_{i,*} = \langle h_{i,1}, h_{i,2}, \dots, h_{i,8} \rangle$ *is an element of* $\{0,1\}^8$ *and* $\mathbf{h}_{i,*} \neq \mathbf{h}_{j,*}$ *for all* $i \neq j$. *Then the Hamming Weight (HW) of exclusive-OR of arbitrary chosen column vectors from H is 0 or 128. In other words,* $HW(\mathbf{h}_{*,j_1} \oplus \mathbf{h}_{*,j_2} \oplus \dots \oplus \mathbf{h}_{*,j_n}) = 0$ *or 128, where n is a random positive integer and* $j_i \in \{1, 2, \dots, 8\}$.

Proof : Let $\mathcal{J}$ be a set of randomly chosen indices from $\{1, 2, \dots, 8\}$. Note that for any duplicated indices α and α' in $\mathcal{J}$, i.e. $\alpha = \alpha'$, removing the duplicated indices from $\mathcal{J}$ makes no change to the result HW.

$$\oplus_{j \in \mathcal{J}} \mathbf{h}_{*,j} = \big(\oplus_{j \in \mathcal{J} - \{\alpha, \alpha'\}} \mathbf{h}_{*,j} \big) \oplus \mathbf{h}_{*,\alpha} \oplus \mathbf{h}_{*,\alpha'}$$

$$= \big(\oplus_{j \in \mathcal{J} - \{\alpha, \alpha'\}} \mathbf{h}_{*,j} \big) \oplus \mathbf{0} = \oplus_{j \in \mathcal{J} - \{\alpha, \alpha'\}} \mathbf{h}_{*,j}.$$

Therefore without loss of generality we can assume that $\mathcal{J}$ contains no duplicated indices and moreover $\big|\mathcal{J}\big| = n \leq 8$.

Now we can define following partitions of indices:

$$\mathcal{I}_{b_1, b_2, \dots, b_n} = \{\ell \in \mathcal{I} | h_{\ell, j_i} = b_i \text{ for all } j_i \in \mathcal{J}\},$$

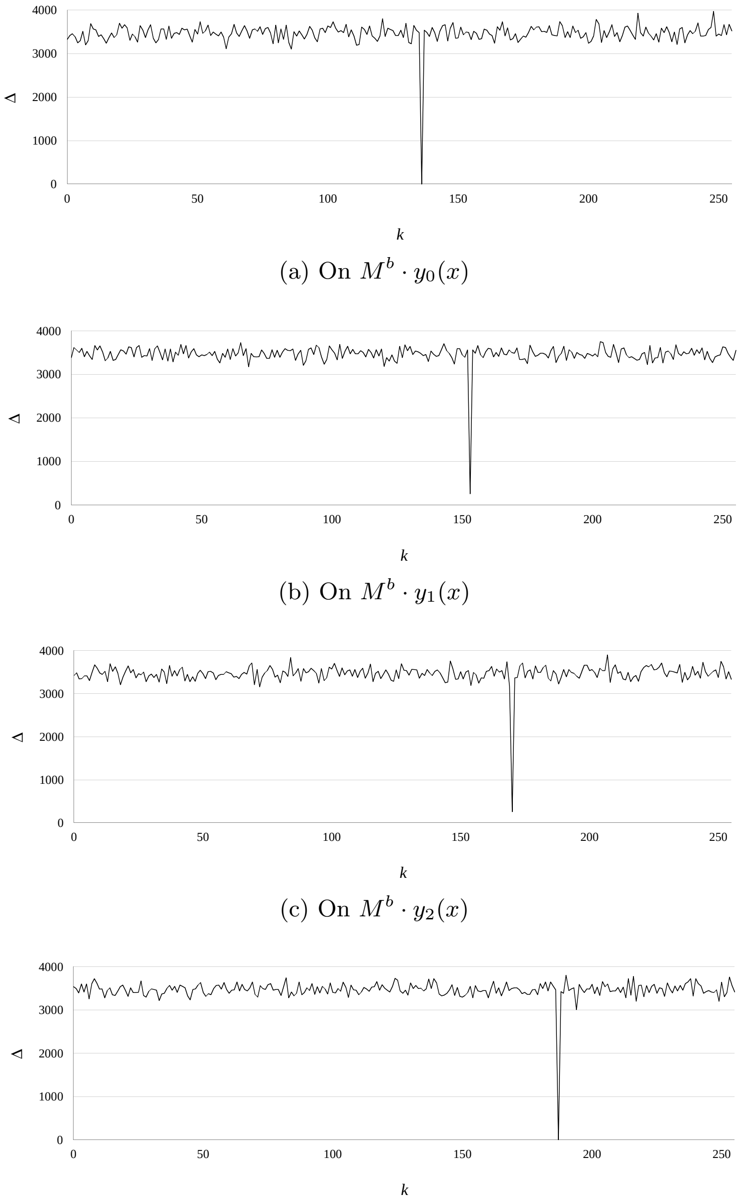

(a) On $M^b \cdot y_0(x)$

(b) On $M^b \cdot y_1(x)$

(c) On $M^b \cdot y_2(x)$

(d) On $M^b \cdot y_3(x)$

Fig. 11: Sum of the imbalance for all key candidates on each $y_{i\in\{0,1,2,3\}}(x)$ multiplied with a balanced matrix.

where $\mathcal{I} = \{1, 2, \ldots, 256\}$. Here all $\mathcal{I}_{b_1,b_2,\ldots,b_n}$ are disjoint to the others and $\cup\mathcal{I}_{b_1,b_2,\ldots,b_n} = \mathcal{I}$.

To complete the proof, we need that for any choice of b_i's, $\left|\mathcal{I}_{b_1,b_2,\ldots,b_n}\right| = 256/2^n = 2^{8-n}$. This can be shown easily as followings. Suppose that $\left|\mathcal{I}_{b_1,b_2,\ldots,b_n}\right| = t > 2^{8-n}$. It means that there are t row vectors in $\mathbf{H}$ satisfying the condition j_i-th bit of the vector equals to b_i. In other words, n bits are determined by choice of b_i's and only $8-n$ bits are remained free. From the condition of t is larger than 2^{8-n} and the pigeon hole principle in mathematics, there must exist at least two indices ℓ and ℓ' in $\mathcal{I}_{b_1,b_2,\ldots,b_n}$ where all bits of $\mathbf{h}_{\ell,*}$ is completely same to the bits of $\mathbf{h}_{\ell',*}$. It contradict to the assumption $\mathbf{h}_{i,*} \neq \mathbf{h}_{j,*}$ for any $i \neq j$.
From the definition of HW, we can deduce $HW(\oplus_{j\in\mathcal{J}}\mathbf{h}_{*,j})$ is summation of $\left|\mathcal{I}_{b_1,b_2,\ldots,b_n}\right|$ where $\oplus_{i=1,\ldots,n}b_i = 1$.

$$\begin{aligned} HW(\oplus_{j\in\mathcal{J}}\mathbf{h}_{*,j}) &= \Sigma_{\oplus_{i=1,\ldots,n}b_i=1}\left|\mathcal{I}_{b_1,b_2,\ldots,b_n}\right| \\ &= \Sigma_{\oplus_{i=1,\ldots,n}b_i=1}2^{8-n} = \Sigma_{2^{n-1}}2^{8-n} \\ &= 2^{n-1}\cdot 2^{8-n} = 2^7 = 128. \end{aligned}$$

Note that if $\mathcal{J}$ is empty after de-duplication then the final HW becomes 0. It concludes the proof of lemma.

Note that $W_{f_i}(w)$ is defined as $\sum_{x\in\{0,1\}^8}(-1)^{f_i(x)\oplus w\cdot x} = \sum_{x\in\{0,1\}^8}(-1)^{M_{i,*}\cdot y(x)\oplus w\cdot x}$, where $M_{i,*}$ is i-th row of the matrix M and $y(x)$ is one of $y_0(x)$ - $y_3(x)$ depending on the target subkey. For convenience, let $y(x) = y_0(x)$, a 32×1 matrix $[2\cdot x \;\; x \;\; x \;\; 3\cdot x]^T$. If we define $\mathbf{Y}(x)$ as a 32×256 matrix with $[2\cdot\mathbf{H} \;\; \mathbf{H} \;\; \mathbf{H} \;\; 3\cdot\mathbf{H}]^T$, where the $\mathbf{H}$ is the matrix defined at the lemma 1. Then the above equation can be re-written as

$$\sum_{j=\{1,2,\ldots 256\}}(-1)^{B_j(M_{i,*}\cdot\mathbf{Y}(x)\oplus(w\cdot\mathbf{H}^T))},$$

where $B_j(v)$ means the j-th bit of the vector v. Since the exponents of the equation can have only two values 0 or 1, the summation over $\{1,2,\ldots,256\}$ can be re-written with the number of exponents which are 1.

$$W_{f_i}(w) = 256 - HW(M_{i,*}\cdot\mathbf{Y}(x)\oplus(w\cdot\mathbf{H}^T))$$

Note that all row vectors of the matrix $\mathbf{Y}(x)$ is represented as summation of row vectors of $\mathbf{H}$. Therefore $M_{i,*}\cdot\mathbf{Y}(x)\oplus(w\cdot\mathbf{H}^T)$ can be also represented as summation of row vectors of $\mathbf{H}$. From the lemma 1, it deduces that the HW of $M_{i,*}\cdot\mathbf{Y}(x)\oplus(w\cdot\mathbf{H}^T)$ is 0 or 128. Finally, $W_{f_i}(w) = 256 - HW(M_{i,*}\cdot\mathbf{Y}(x)\oplus(w\cdot\mathbf{H}^T))$ becomes 256 or 0. What is remarkable point over here is that the probability of $W_{f_i}(w) = 256$ is very small but not zero. Specifically, it happens when all row indices of $\mathbf{H}$ are canceled each other when the summation is computed with the randomly chosen matrix M.
As mentioned already, our experiment showed that $W_{f_i}(w) = 256$ with 0.3% in the calculation with the correct key, while the wrong key candidates produced $|W_{f_i}(\omega)| = 56$ at maximum and 13.13 in average. For this reason, 1024 tests of $W_{f_i}(w)$ for a subkey recovery have been successful with overwhelming probability.

4 Proposed Method

Our analysis in the previous section shows that well-balanced distribution of the intermediate values are the main reason behind the key leakage. In order to make it unbalanced, our key idea is to insert random bytes in the intermediate values before linear transformations. From now on, we answer to the following questions.

- Where is the appropriate position for random bytes to be inserted?
- How many random bytes must be inserted?
- How to apply this key idea to a new WB-AES implementation?

We begin with an analysis of the inserting position and the required number of random bytes to be inserted.

4.1 Inserting A Random Byte in the Intermediate Values

First, we will insert a random byte at a particular position in the 4-byte intermediate value $y_{i\in\{0,1,2,3\}}(x)$ and then perform a linear transformation with a 40×40 binary block invertible matrix M^* to check if any key leakage occurs. Among the five inserting positions ρ_1 - ρ_5 of y_0, for example,

$$\left[\rho_1 \ 2\cdot x \ \rho_2 \ x \ \rho_3 \ x \ \rho_4 \ 3\cdot x \ \rho_5\right]^T$$

we select ρ_i, where $i \in$ [1, 5], and then insert different $\gamma \in_R$ GF(2^8) at ρ_i for each $x \in$ GF(2^8). Let $y_0^*(x)$ denote $y_0(x)$ after the random byte insertion, and $f^*(x)$ denote $y_0^*(x) \cdot M^*$. Then we can define the Walsh transforms with respect to f^*:

$$W_{f_i^*}(\omega) = \Sigma_{x\in\{0,1\}^8}(-1)^{f_i^*(x)\oplus x\cdot\omega}$$

for 40 Boolean functions

$$f^*_{i\in\{1,\ldots,40\}}(x) : \{0,1\}^8 \to \{0,1\}.$$

With 1000 randomly generated M^*, we computed $W_{f_i^*}(\omega)$ with respect to y_0 - $y_3(x)$ for each position ρ_i. As a result, TABLE 2 gives us that the correct key results in $W_{f_i^*}(\omega) = 0$ with approximately 5% and the average $|W_{f_i^*}(\omega)|$ is about 12.7. Recall that, without the random byte insertion, $W_{f_i}(\omega) = 0$ with approximately 99.7% and the average of $|W_{f_i}(\omega)|$ is approximately 0.7.
To see the effect of the random byte insertion, we conducted the additional experiment as follows.

1. Let $y^\gamma(x) = [\gamma 1 \ \gamma 2 \ \gamma 3 \ \gamma 4 \ \gamma 5]^T$ for each $x \in$ GF(2^8). In other words, replace all the key-dependent intermediate values with random bytes.
2. $f^\gamma(x) = M^* \cdot y^\gamma(x)$.
3. Repeat step (1) - (2) with 1000 random M^* matrices, and accumulate the number of occurrences of each value of $W_{f_i^\gamma}(\omega)$.
4. Compute % of $W_{f_i^\gamma}(\omega) = 0$ and the average $|W_{f_i^\gamma}(\omega)|$.

	ρ_1	ρ_2	ρ_3	ρ_4	ρ_5
% of $W_{f_i^*}(\omega) = 0$	5.05 (0.03)	5.06 (0.07)	4.93 (0.05)	5.0 (0.05)	5.04 (0.04)
Average of $\lvert W_{f_i^*}(\omega)\rvert$	12.73 (0.02)	12.75 (0.01)	12.76 (0.01)	12.73 (0.01)	12.76 (0.01)
Similarity with $W_{f_i^\gamma}$	> 0.999				

Table 2: $W_{f_i^*}$ after inserting a random byte at each inserting position (the standard deviation in parenthesis), and the cosine similarity of the distributions between $W_{f_i^*}$ and $W_{f_i^\gamma}$.

5. Compute the cosine similarity between the distributions of $W_{f_i^\gamma}(\omega)$ and $W_{f_i^*}(\omega)$ for each of y_0 - y_3 and for each ρ_i.

As a result, we have $W_{f_i^\gamma}(\omega) = 0$ with approximately 5%, the average $|W_{f_i^\gamma}(\omega)|$ is approximately 12.74, and the cosine similarity between their distributions is always larger than 0.999. The cosine similarity larger than 0.99 means they show very similar distribution. We note that the cosine similarity between the distributions of $W_{f_i^\gamma}(\omega)$ and $W_{f_i}(\omega)$ is about 0.25.

In order to visualize this effect of inserting a random byte, we select ρ_5 and calcalculate the sum of the imbalances of $W_{f_i^*}(\omega)$ for each key candidate with ω such that $\mathrm{HW}(\omega) = 1$, as follows:

$$\Delta^{f^*}_{k\in\{0,1\}^8} = \sum_{\omega=1,2,\ldots,128} \sum_{i=1,\ldots,40} |W_{f_i^*}(\omega)|,$$

Fig. 12 shows $\Delta^{f^*}_{k\in\{0,1\}^8}$ and we can see that the correct subkeys *0x*88 - *0x*BB are no longer distinguishable from other candidates.

In addition, it is noticeable that inserting more than two random bytes in the intermediate values does not increase the imbalance; they show a similar level of the imbalance of the one-byte insertion. Thus, we can conclude that inserting a random byte into anywhere among ρ_1-ρ_5 can effectively prevent the key leakage of the linear transformation. Based on all the analysis, we explain how to implement a key leakage preventive WB-AES algorithm with 128-bit key size in the following.

4.2 Secure WB-AES Implementation

In this section, we explain how to apply the random byte insertion before linear transformations in order to protect the first and final rounds of WB-AES. Note that any attack on the inner rounds which require large complexity of 2^{128} key candidates is not practical. Our WB-AES uses the table name (number) used in previous studies to minimize confusion but only mark * in its superscript at the beginning of the name if we modify its structure or size. Then, a set of lookup tables in our proposed WB-AES is basically composed of four types: **TypeII*,

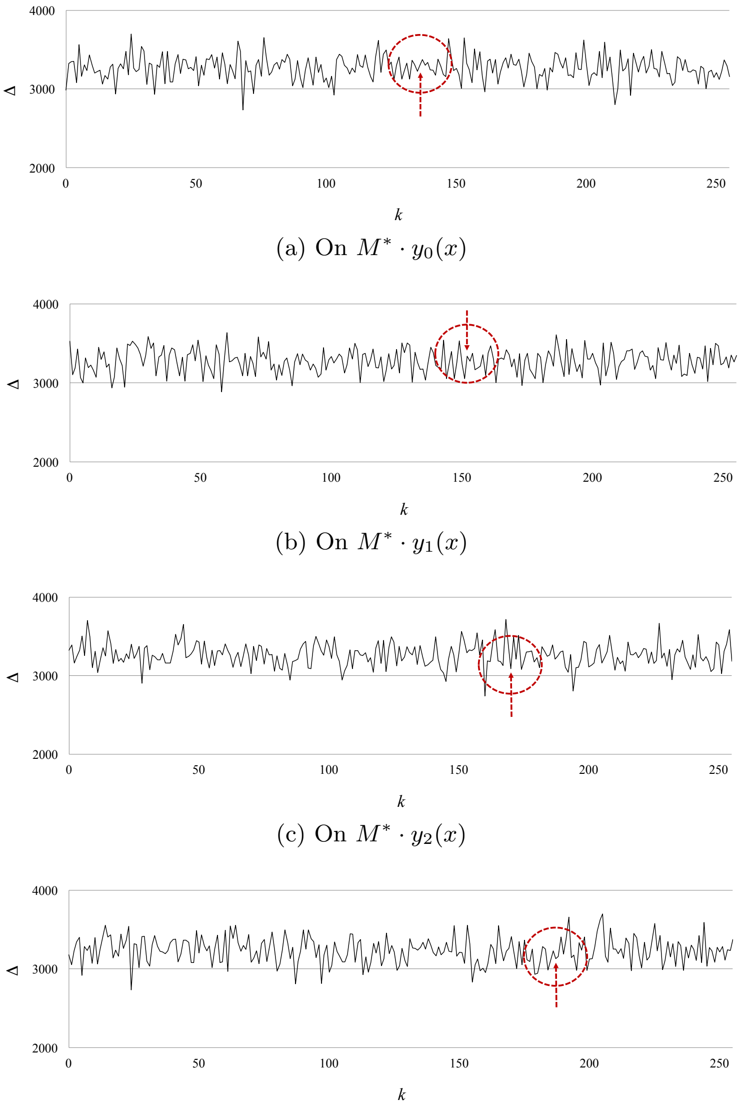

(a) On $M^* \cdot y_0(x)$

(b) On $M^* \cdot y_1(x)$

(c) On $M^* \cdot y_2(x)$

(d) On $M^* \cdot y_3(x)$

Fig. 12: Sum of the imbalance of $W_{f_i^*}(\omega)$ for all key candidates. Red arrow: the correct key.

**TypeIII*, **TypeIV* and *TypeV*.

***TypeII**. We begin by the connection with x and y used in the previous sections. In the non-protected WB-AES implementation (Section 2), the linear transformation is applied to Ty_i during the *TypeII* generation. In our WB-AES, we pick

$\gamma \in_R$ GF(2^8) for each $x \in$ GF(2^8), and define $Ty^*(x)$:

$$\begin{aligned} Ty_0^*(x) &= [2x\ x\ x\ 3x\ \gamma \in_R GF(2^8)]^T \\ Ty_1^*(x) &= [3x\ 2x\ x\ x\ \gamma \in_R GF(2^8)]^T \\ Ty_2^*(x) &= [x\ 3x\ 2x\ x\ \gamma \in_R GF(2^8)]^T \\ Ty_3^*(x) &= [x\ x\ 3x\ 2x\ \gamma \in_R GF(2^8)]^T. \end{aligned}$$

The next step is to perform linear transformations on $Ty_i^*(x)$ with M^* and apply non-linear transformations as illustrated in Fig 13 and Algorithm 1. Note that the input decoding from round 2 takes into account the index change due to ShiftRows. During the execution of WB-AES, its lookup values will contain 5-byte outputs including an encoded random byte and thus the intermediate values after visiting **TypeII* will be store in a 5×4×4 matrix.

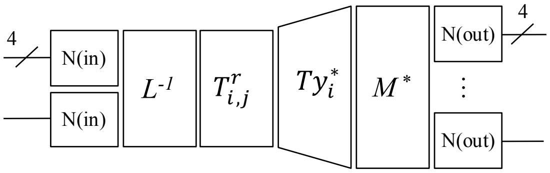

Fig. 13: A schematic diagram of **TypeII* generation.

***TypeIII**. During the **TypeIII* generation shown in Fig. 14, we perform the inverse linear transformation with $(M^*)^{-1}$ and apply the linear transformation with L. Now we need 180 (=9×5×4) 8×8 binary invertible matrices $L^r_{i,j}$, where $r \in [1, 9]$, $0 \le i \le 4$, and $0 \le j \le 3$ because **TypeIII* gives an additional byte in the intermediate values. Algorithm 2 describes the generation of **TypeIII.* After visiting **TypeIII*, we have the intermediate values in a 5×4×5 matrix.

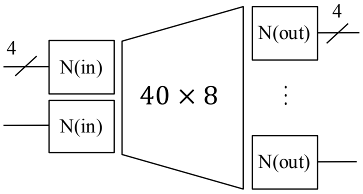

Fig. 14: A schematic diagram of **TypeIII* generation.

***TypeIV**. **TypeIV_II* and **Type IV_III* are used to XOR the lookup values of **TypeII* and **TypeIII*, respectively. **TypeIV_II* combines 5×4×4 intermediate

```
for $r = 0$ to $8$ do
    for $i = 0$ to $3$ do
        for $j = 0$ to $3$ do
            for $p' = 0$ to $255$ do
                if $r == 0$ then
                    $p = p'$;
                else
                    $\{i,\, j'\} = \{i,\, (j+i) \bmod 4\ \}$
                    $p' =$ inverse-non-linear-transform($p'$)
                    $p = (L^{r-1}_{i,j'})^{-1} \cdot p'$
                end
                $x = T^{r}_{i,j}(p)$
                $y = Ty_i(x)$
                $y^* = y \mid\mid \gamma \in_R \mathrm{GF}(2^8)$
                $f^* = M^* \cdot y^*$
                for $k = 0$ to $4$ do
                    $f^*[k] =$ non-linear-transform($f^*[k]$)
                    $^*TypeII^{r}_{i,j,p',k} = f^*[k]$
                end
            end
        end
    end
end
```

Algorithm 1: **TypeII* Generation.

```
for $r = 0$ to $8$ do
    for $i = 0$ to $4$ do
        for $j = 0$ to $3$ do
            for $p' = 0$ to $255$ do
                $p =$ inverse-non-linear-transform($p'$)
                $g^*[5] = \{0, 0, 0, 0, 0\}$
                $g^*[i] = p$
                $g^* = (M^*)^{-1} \cdot g^*$
                for $k = 0$ to $4$ do
                    $g^* = L^{r}_{k,j} \cdot g^*$
                    $g^*[k] =$ non-linear-transform($g^*[k]$)
                    $^*TypeIII^{r}_{i,j,p',k} = g^*[k]$
                end
            end
        end
    end
end
```

Algorithm 2: **TypeIII* Generation.

values into a 5×4 state matrix and *$TypeIV\_III$* combines 5×4×5 intermediate values into a 5×4 state matrix. We extract the first four rows of this resulting 5×4 intermediate matrix into a 4×4 state matrix and use it as the next round input. Fig. 15 and Fig. 16 simplify the lookup flows of *$TypeIV$ following *$TypeII$ and *$TypeIII$.

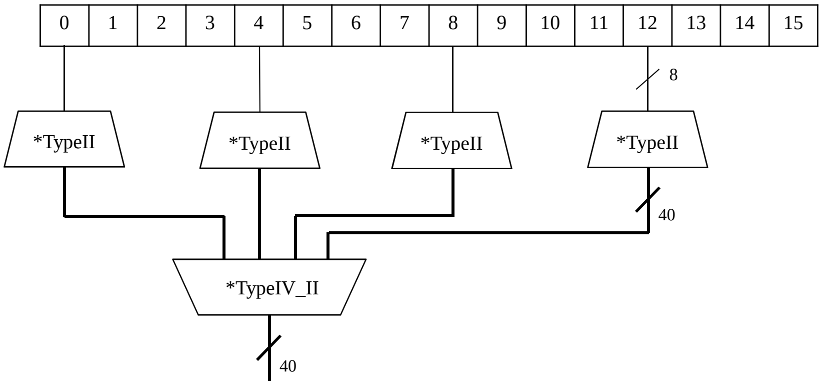

Fig. 15: *$TypeII$ and *$TypeIV\_II$ lookups.

By using *$TypeII$, *$TypeIV\_II$, *$TypeIII$, and *$TypeIV\_III$ in the first round, we can protect against gray-box attacks using SubBytes outputs on *$TypeII$ lookup values. Next, we explain how to protect the first round output and final round input.

4.3 More Protection and Our Variants

As explained in Section 2, there can be three key leakage points in WB-AES. It is noticeable that the higher the security level, the higher the cost for a white-box cryptographic implementation. In this point of view, the authors in [10] proposed three different variants of masked WB-AES implementations, aptly named CASE 1, 2 and 3, depending on the explained attack complexity.

- CASE 1: Protecting first round *TypeII* outputs
- CASE 2: CASE 1 + protecting the whole final round
- CASE 3: CASE 2 + protecting the whole first round.

So far, we have introduced our method to protect *TypeII* outputs in the first round. Our WB-AES of inserting a random byte before linear transformations protects *$TypeII$ and *$TypeIV\_II$ outputs, but does not provide any protection on each round output since combining the intermediate values by *$TypeIV\_III$

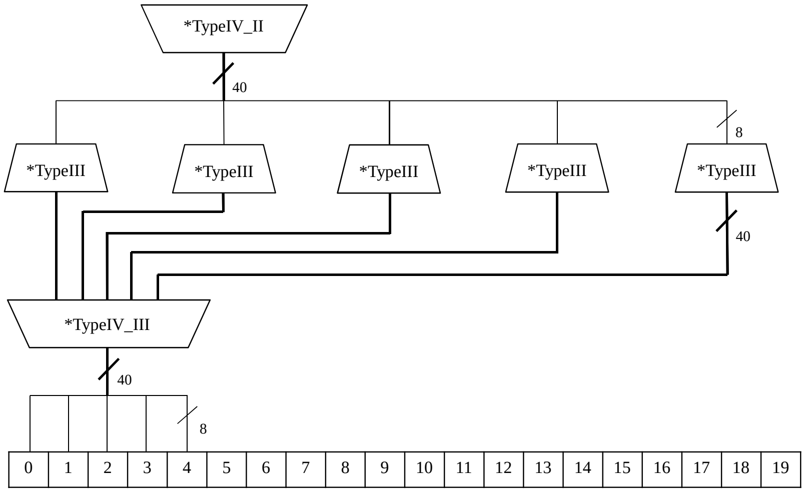

Fig. 16: **TypeIII* and **TypeIV_III* lookups.

cancels out the linear transformation by M^* and apply another linear transformation by L on each byte of the round output. As a result, attacks on **TypeIV_III* are still possible, and thus the remaining task is to protect the final round input and the first round output.

Suppose that we apply the same technique of a random byte insertion a 16×16 invertible matrix L^*. This choice leads to the following additional costs:

- The **TypeIII* size increases.
- The **TypeIV_III* size increases.
- A temporary storage for intermediate values increases.
- The number of table lookup increases.
- A 16-bit to 8-bit mapping table is needed to cancel out L^* and apply L corresponding to the **TypeII* input decoding in the next round; the mapping table should be protected by a secure non-linear transformation with 8-bit to 8-bit random bijections.

Due to these additional costs, it is cost effective to partially adapt 8-bit to 8-bit random bijections at the end of **TypeIV_III* like *TypeIV_IIIC* used in [10], rather than inserting a random byte in **TypeIII*. More specifically, an XOR lookup table using 8-bit to 8-bit random bijections based non-linear transformations requires the same size with the 16-bit to 8-bit mapping table, but there will be no additional costs imposed at **TypeIII* and table lookups.

Let us have three variants of CASE 1, 2, and 3 like in the case of the masked WB-AES variants. Then we already have the CASE 1 implementation including **TypeII*, **TypeIII*, and **TypeIV* in the first round.

Next, we describe how to implement the CASE 2 implementation. We append a postfix 'N' to the end of **TypeIV_III* indicating the use of 8-bit to 8-bit random bijections for non-linear transformations. Fig. 17 shows a diagram of **TypeIV_IIIN*, and Fig. 18 provides a simple lookup flow of **TypeIII*, **TypeIV_III* and **TypeIV_IIIN* to produce the final round input at the ninth round. Then the inverse non-linear transformation used in **TypeVN* generation must be the corresponding inverse 8-bit to 8-bit bijections as shown in Fig. 19

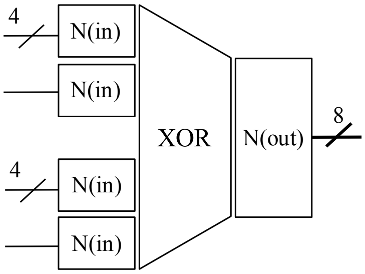

Fig. 17: A schematic diagram of **TypeIV_IIIN* generation.

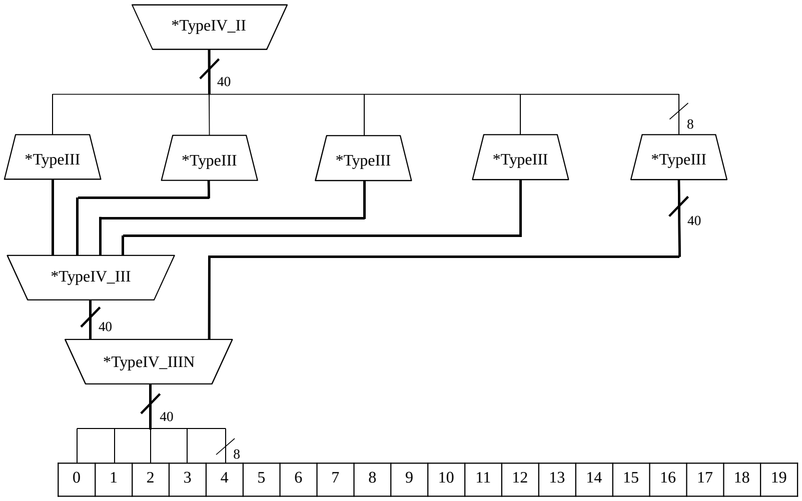

Fig. 18: **TypeIV_III* and **TypeIV_IIIN* lookups.

In the CASE 3 implementation, **TypeIV_IIIN* is used in the first round and thus **TypeIIN* in the second round must have the corresponding 8-bit to 8-bit inverse bijections as shown in Fig. 20. Note that a random byte insertion is not applied to **TypeIIN* because this gives the inner round intermediate values

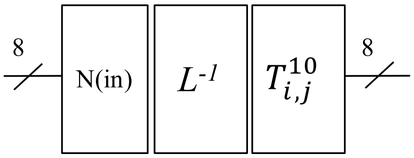

Fig. 19: A schematic diagram of **TypeVN* generation.

which require an attacker to completely know the first round key. Then the table lookup sequences for each variant are given in Fig. 21.

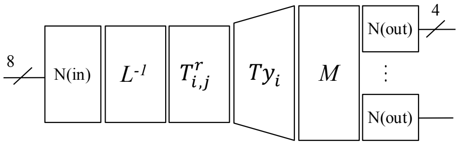

Fig. 20: A schematic diagram of **TypeIIN* generation.

5 Evaluation

In this section, we evaluate the security and performance of our proposed method. To verify the key leakage protection, we use the Walsh transform and DCA attacks. The performance evaluation compares the lookup table size and the number of lookups of WB-AES with the initial WB-AES and the masked WB-AES implementations [5][10].

5.1 Security

We demonstrate the prevention of key leakages from **TypeII* and **TypeIV_IIIN* in our WB-AES implementation. For the 8^{th} subkey and attacker's hypothetical SubBytes output x, let 40 Boolean functions $f^*_{i\in\{1,\ldots,40\}}(x)$: $\{0,1\}^8 \rightarrow \{0,1\}$ denote **TypeII* lookup values in the first round. Then we have the sum of imbalance:

$$\Delta^{f^*}_{k\in\{0,1\}^8} = \sum_{\omega=1,2,\ldots,128} \sum_{i=1,\ldots,40} |W_{f_i}(\omega)|,$$

where $\mathrm{HW}(\omega) = 1$. We can see there is no longer distinguishable peak at the right subkey ($0x88$) in Fig. 23a. This gives us that power analysis such as DPA and CPA as well as DCA attacks using the SubBytes output in the first round will not be successful on our WB-AES implementation. In order to show the DCA result, we collected 1,000 software execution traces by DCA techniques and then

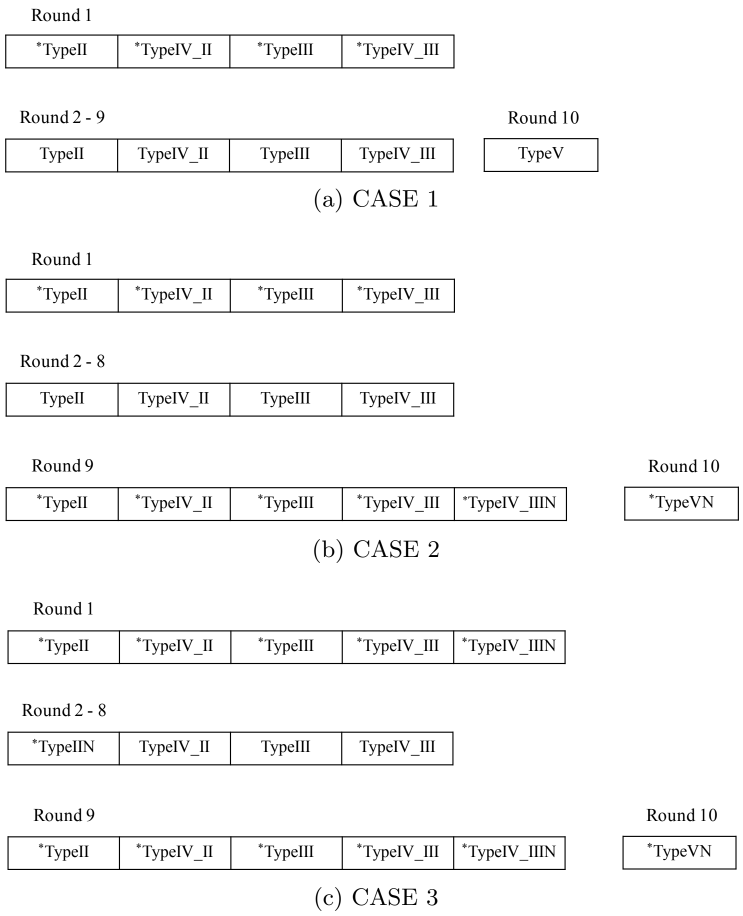

(a) CASE 1

(b) CASE 2

(c) CASE 3

Fig. 21: Table lookup sequences in the CASE 1-3 implementations.

performed a CPA attack. TABLE 3 shows DCA was not able to recover any key from our WB-AES, and the last two rows provide the highest correlation coefficient and the correct key's correlation coefficient values, respectively. We know that the coefficient value around 0.2 of the correct key means that there is no meaningful correlation between correct hypothetical values and lookup values.

In addition, we conducted the same experiment as in Sectin 2 with the attacker's hypothetical input value x and 8 Boolean functions $f_{i\in\{1,\ldots,8\}}(x)$: $\{0,1\}^8 \rightarrow \{0,1\}$ for the encoded final round input so that we verify the key leakage prevention at **TypeIV_IIIN* outputs. As a result, there is no peak at the right key candidate ($0x13$) as shown in Fig. 23b.

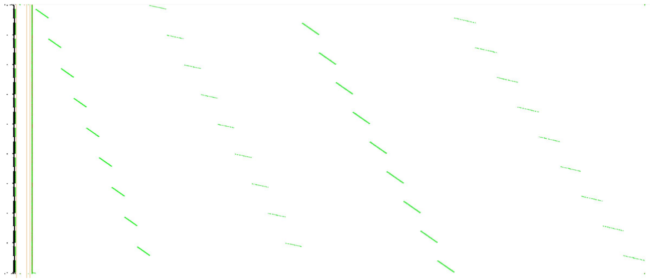

Fig. 22: Visualization of a software execution trace of our WB-AES implementation. Green: read memory addresses, Red: write memory address.

Table 3: DCA ranking for our WB-AES implementation when conducting monobit CPA on the SubBytes output in the first round with 1000 software traces.

SubKey TargetBit	1	2	3	4	5	6	7	8	9	10	11	12	13	14	15	16
1	211	105	33	180	126	226	93	225	251	176	67	230	129	130	150	172
2	256	150	250	13	126	20	212	25	110	200	162	71	77	159	76	192
3	11	59	28	154	232	139	86	67	171	85	205	197	106	114	96	245
4	71	161	52	4	138	249	37	19	36	189	220	121	34	25	31	101
5	219	41	249	237	172	93	112	255	199	191	15	103	140	90	94	158
6	154	246	143	53	135	159	48	229	99	5	32	98	251	149	207	179
7	165	167	237	50	238	185	156	208	127	54	56	157	145	59	70	251
8	253	199	248	173	122	208	186	208	129	56	43	110	113	202	69	92
Highest coeff.	0.33	0.29	0.29	0.28	0.29	0.30	0.31	0.28	0.29	0.30	0.30	0.35	0.30	0.31	0.33	0.30
Key's coeff.	0.22	0.19	0.20	0.25	0.16	0.21	0.20	0.21	0.19	0.24	0.23	0.18	0.19	0.21	0.21	0.17

5.2 Performance

Our performance evaluation in this section compares the total lookup table size and the number of table lookups with the initial WB-AES and masked WB-AES implementations [5][10].

Table size. Before table size comparsions, we need to mention two things: 1) Because there is no variant in the initial WB-AES implementation, we denote it CASE 1 (without CASE 2 and CASE 3) for convenient comparison with the masked WB-AES and our WB-AES implementations; 2) It is necessary to recalculate the masked WB-AES table size and table lookups for the pair comparison because the authors calculated for the case of their masking technique applied to both outer and inner rounds while we applied our technique to only outer rounds. Thus, we compare with their reduced sizes of protecting only outer rounds.
The table size of CASE 1 is 544,768 bytes in total and this is calculated as follows:

- * *TypeII*: 4×4×256×5 = 20,480

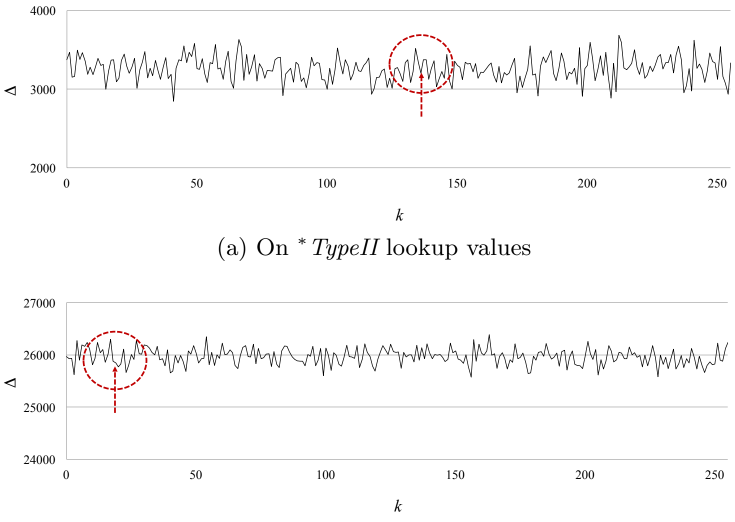

(a) On **TypeII* lookup values

(b) On **TypeVN* input values

Fig. 23: Sum of the imbalance for all key candidates in our WB-AES.

- **TypeIV_II*: 5×4×3×2×128 = 15,360
- **TypeIII*: 5×4×256×5 = 25,600
- **TypeIV_III*: 5×4×4×2×128 = 20,480
- *TypeII*: 8×4×4×256×4 = 131,072
- *TypeIII*: 8×4×4×256×4 = 131,072
- *TypeIV*: 2×8×4×4×3×2×128 = 196,608
- *TypeV*: 4×4×256 = 4,096 bytes.

In CASE 2, the total size is 1,874,944 bytes computed by rewriting the table size in the final round as follows:

- **TypeII*: 4×4×256×5 = 20,480
- **TypeIV_II*: 5×4×3×2×128 = 15,360
- **TypeIII*: 5×4×256×5 = 25,600
- *TypeIV_III*: 5×4×3×2×128 = 15,360
- **TypeIV_IIIN*: 5×4×256×256 = 1,310,720.

Lastly, the total size of CASE 3 is 3,180,544 bytes computed by rewriting the **TypeIV_III* size in the first round as follows:

- **TypeIV_III*: 5×4×3×2×128 = 15,360
- **TypeIV_IIIN*: 5×4×256×256 = 1,310,720.

TABLE 4 shows the comparisons with the previous implementations. Our WB-AES implementation reduces approximately 33% of the memory requirements of masked WB-AES in CASE 2 and CASE 3.

	CASE 1	CASE 2	CASE 3
Initial WB-AES	520,192	-	-
Masked WB-AES	548,864	2,774,688	4,763,648
Our WB-AES	544,768	1,874,944	3,180,544

Table 4: Table size comparison (byte) with the previous WB-AES implementations.

Table lookup. The number of table lookups of CASE 1 is 2124 in total and this is calculated as follows:

- **TypeII*: 4×4 = 16
- **TypeIV_II*: 5×4×3×2 = 120
- **TypeIII*: 5×4 = 20
- **TypeIV_III*: 5×4×4×2 = 160
- *TypeII*: 8×4×4 = 128
- *TypeIII*: 8×4×4 = 128
- *TypeIV*: 2×8×4×4×3×2 = 1536
- *TypeV*: 4×4 = 16.

In addition, the numbers of lookups in CASE 2 and CASE 3 are 2196 and 2176. Here, the use of 8-bit to 8-bit bijections in the XOR tables slightly reduces the number of lookups. Compared to the masked implementations, our WB-AES requires slightly less table lookups. We note that the initial WB-AES and our WB-AES implementations require 10 ShiftRows while the masked WB-AES implementation needs 11 ShiftRows (for the mask state matrix) in total.

	CASE 1	CASE 2	CASE 3
Initial WB-AES	2,032	-	-
Masked WB-AES	2,176	2,288	2,256
Our WB-AES	2,124	2,196	2,176

Table 5: Table lookup comparison with the previous WB-AES implementations.

In summary, our WB-AES implementation can prevent key leakages with at most 33 percent less memory requirements than the masked implementations. We remark that the white-box cryptographic applications have been limited due to the high memory requirements that mainly determine the cost. For this reason, the reduced table size can contribute to the widespread use of white-box cryptography.

6 Conclusion and Discussion

In this paper, our analysis shows the well distributed intermediate values cause the key leakage after linear transformation in the white-box implementation. Based on this analysis, we introduce a method of inserting a random byte into intermediate values before linear transformations to prevent key leakages and propose a WB-AES implementation using this principle. To protect the outer round output, we partially apply non-linear transformations using 8-bit to 8-bit random bijections and provide three different variants of WB-AES depending on the security levels. In conclusion, our WB-AES, as a non-masking implementation, does not require any static or dynamic random source and decreases the memory requirement by at most 33% with slightly reduced table lookups, compared to the masked WB-AES.

References

1. Billet, O., Gilbert, H., Ech-Chatbi, C.: Cryptanalysis of a White Box AES Implementation. In: Selected Areas in Cryptography, 11th International Workshop, SAC 2004, Waterloo, Canada, August 9-10, 2004, Revised Selected Papers. pp. 227–240 (2004), http://dx.doi.org/10.1007/978-3-540-30564-4_16
2. Bos, J.W., Hubain, C., Michiels, W., Teuwen, P.: Differential Computation Analysis: Hiding your White-Box Designs is Not Enough. vol. 2015, p. 753 (2015), http://dblp.uni-trier.de/db/journals/iacr/iacr2015.html#BosHMT15
3. Brier, E., Clavier, C., Olivier, F.: Correlation Power Analysis with a Leakage Model. In: Cryptographic Hardware and Embedded Systems - CHES 2004: 6th International Workshop Cambridge, MA, USA, August 11-13, 2004. Proceedings. Lecture Notes in Computer Science, vol. 3156, pp. 16–29. Springer (2004)
4. Bringer, J., Chabanne, H., Dottax, E.: White Box Cryptography: Another Attempt. IACR Cryptology ePrint Archive 2006, 468 (2006), http://eprint.iacr.org/2006/468
5. Chow, S., Eisen, P., Johnson, H., Oorschot, P.C.V.: White-Box Cryptography and an AES Implementation. In: Proceedings of the Ninth Workshop on Selected Areas in Cryptography (SAC 2002). pp. 250–270. Springer-Verlag (2002)
6. Chow, S., Eisen, P.A., Johnson, H., van Oorschot, P.C.: A White-Box DES Implementation for DRM Applications. In: Security and Privacy in Digital Rights Management, ACM CCS-9 Workshop, DRM 2002, Washington, DC, USA, November 18, 2002, Revised Papers. pp. 1–15 (2002), http://dx.doi.org/10.1007/978-3-540-44993-5_1
7. Goubin, L., Masereel, J., Quisquater, M.: Cryptanalysis of White Box DES Implementations. In: Selected Areas in Cryptography, 14th International Workshop, SAC 2007, Ottawa, Canada, August 16-17, 2007, Revised Selected Papers. pp. 278–295 (2007), http://dx.doi.org/10.1007/978-3-540-77360-3_18
8. Karroumi, M.: Protecting White-Box AES with Dual Ciphers. In: Information Security and Cryptology - ICISC 2010 - 13th International Conference, Seoul, Korea, December 1-3, 2010, Revised Selected Papers. pp. 278–291 (2010), http://dx.doi.org/10.1007/978-3-642-24209-0_19
9. Kocher, P.C., Jaffe, J., Jun, B.: Differential Power Analysis. In: Advances in Cryptology - CRYPTO '99, 19th Annual International Cryptology Conference, Santa

Barbara, California, USA, August 15-19, 1999, Proceedings. pp. 388–397 (1999), http://dx.doi.org/10.1007/3-540-48405-1_25

10. Lee, S., Kim, T., Kang, Y.: A Masked White-Box Cryptographic Implementation for Protecting Against Differential Computation Analysis. IEEE Transactions on Information Forensics and Security 13(10), 2602–2615 (Oct 2018)
11. Lee, S., Choi, D., Choi, Y.J.: Conditional Re-encoding Method for Cryptanalysis-Resistant White-Box AES. vol. 5. Electronics and Telecommunications Research Institute (Oct 2015), http://dx.doi.org/10.4218/etrij.15.0114.0025
12. Lepoint, T., Rivain, M., Mulder, Y.D., Roelse, P., Preneel, B.: Two Attacks on a White-Box AES Implementation. In: Selected Areas in Cryptography - SAC 2013 - 20th International Conference, Burnaby, BC, Canada, August 14-16, 2013, Revised Selected Papers. pp. 265–285 (2013), http://dx.doi.org/10.1007/978-3-662-43414-7_14
13. Link, H.E., Neumann, W.D.: Clarifying Obfuscation: Improving the Security of White-box DES. In: International Conference on Information Technology: Coding and Computing (ITCC'05) - Volume II. vol. 1, pp. 679–684 Vol. 1 (April 2005)
14. Mangard, S., Oswald, E., Popp, T.: Power Analysis Attacks: Revealing the Secrets of Smart Cards (Advances in Information Security) (2007)
15. Michiels, W., Gorissen, P., Hollmann, H.D.L.: Cryptanalysis of a Generic Class of White-Box Implementations. In: Selected Areas in Cryptography, 15th International Workshop, SAC 2008, Sackville, New Brunswick, Canada, August 14-15, Revised Selected Papers. pp. 414–428 (2008), http://dx.doi.org/10.1007/978-3-642-04159-4_27
16. Mulder, Y.D., Roelse, P., Preneel, B.: Cryptanalysis of the Xiao - Lai White-Box AES Implementation. In: Selected Areas in Cryptography, 19th International Conference, SAC 2012, Windsor, ON, Canada, August 15-16, 2012, Revised Selected Papers. pp. 34–49 (2012), http://dx.doi.org/10.1007/978-3-642-35999-6_3
17. Mulder, Y.D., Wyseur, B., Preneel, B.: Cryptanalysis of a Perturbated White-Box AES Implementation. In: Progress in Cryptology - INDOCRYPT 2010 - 11th International Conference on Cryptology in India, Hyderabad, India, December 12-15, 2010. Proceedings. pp. 292–310 (2010), http://dx.doi.org/10.1007/978-3-642-17401-8_21
18. Sanfelix, E., Mune, C., de Haas, J.: Unboxing the White-Box: Practical Attacks against Obfuscated Ciphers. In: Presented at BlackHat Europe 2015 (2015), https://www.blackhat.com/eu-15/briefings.html
19. Sasdrich, P., Moradi, A., Güneysu, T.: White-Box Cryptography in the Gray Box - - A Hardware Implementation and its Side Channels -. In: Fast Software Encryption - 23rd International Conference, FSE 2016, Bochum, Germany, March 20-23, 2016, Revised Selected Papers. pp. 185–203 (2016), http://dx.doi.org/10.1007/978-3-662-52993-5_10
20. Wyseur, B.: White-Box Cryptography. In: Encyclopedia of Cryptography and Security, 2nd Ed. pp. 1386–1387 (2011), http://dx.doi.org/10.1007/978-1-4419-5906-5_627
21. Wyseur, B., Michiels, W., Gorissen, P., Preneel, B.: Cryptanalysis of White-Box DES Implementations with Arbitrary External Encodings. In: Selected Areas in Cryptography, 14th International Workshop, SAC 2007, Ottawa, Canada, August 16-17, 2007, Revised Selected Papers. pp. 264–277 (2007), http://dx.doi.org/10.1007/978-3-540-77360-3_17
22. Xiao, J., Zhou, Y.: Generating Large Non-Singular Matrices over an Arbitrary Field with Blocks of Full Rank (2002), http://eprint.iacr.org/2002/096

23. Xiao, Y., Lai, X.: A Secure Implementation of White-box AES. In: The Second Internationial Conference on Computer Science and Its Applications - CSA 2009. vol. 2009, pp. 1–6 (2009)